

# In Situ Patterning of Organic Single-Crystalline Nanoribbons on a SiO<sub>2</sub> Surface for the Fabrication of Various Architectures and High-Quality Transistors\*\*

By Qingxin Tang, Hongxiang Li, Yabin Song, Wei Xu, Wenping Hu\*, Lei Jiang, Yunqi Liu, Xiangke Wang, and Daoben Zhu\*

Nanowires and nanoribbons can act as both active devices and interconnectors, and are regarded as a “bottom-up” paradigm of nanoelectronics. For example, a crossed nanowire or nanoribbon architecture enables diverse functions simply through the careful choice of the nanowire or nanoribbon building blocks, and provides possibilities for scalable integration at high densities. Hence, the synthesis and patterning of nanowires and nanoribbons has attracted particular attention in recent years. This is especially true for single-crystalline nanowires and nanoribbons because single crystals can reveal the intrinsic properties of the materials and open up possibilities for high-quality devices and circuits. Though extensive studies have been focused on carbon nanotubes as well as nanowires and nanoribbons made from inorganic semiconductors, little work has addressed 1D single crystals of organic semiconductors. In this work, using a typical organic semiconductor, copper phthalocyanine (CuPc), we demonstrate a novel method for the in situ patterning of organic single-crystalline nanoribbons on an SiO<sub>2</sub> surface to obtain various

architectures. A series of organic field-effect transistors (OFETs) based on patterned nanoribbons were fabricated, exhibiting low threshold voltages and high carrier mobilities. The high transistor performance comes about because the in situ patterning process is free from surface pollution and crystal damage, and the process provides an intimate contact between the nanoribbon and the SiO<sub>2</sub> at the semiconductor/insulator interface. This is a promising method for the fabrication of nanoarchitectures or nanodevices from organic single crystals on conventional SiO<sub>2</sub>/Si substrates.

Recently, the field of organic electronics has been attracting worldwide attention and experiencing rapid development.<sup>[1]</sup> As basic elements of organic electronics, OFETs are the topic of many studies. OFETs based on single crystals<sup>[2]</sup> are especially interesting because they show intrinsic charge-transport properties and high mobility because of the absence of grain boundaries in single crystals. Some organic crystals<sup>[2]</sup> exhibit a mobility higher than 1 cm<sup>2</sup> V<sup>-1</sup> s<sup>-1</sup>, which is comparable to or even better than that of amorphous silicon. Nevertheless, there are still many factors limiting the applications of OFETs. One challenging task is the handling of such fragile crystals.<sup>[3]</sup> Currently, there are two main approaches for the fabrication of single-crystal devices: the “electrostatic bonding” method<sup>[4]</sup> and the “direct” device fabrication method.<sup>[5]</sup> In both cases single crystals must be handpicked and made into an individual device. The handpicking process can easily cause crystal surface pollution and crystal damage, resulting in lower performance of the device and very low reproducibility. Furthermore, it is hard to imagine the fabrication of various architectures using organic single crystals, or the fabrication of devices using very small organic crystals, for example, nanocrystals, through this handpicking process.

To overcome the disadvantages of the handpicking process it is desirable to grow single crystals directly on the gate insulator. Clearly, if single crystals could be grown on the surface of the gate insulator and be in tight contact with the insulator, the process of device fabrication would be greatly simplified. Moreover, if the contact between the crystal and insulator surface was intimate enough, the crystal/insulator interface would have less opportunity to be polluted or damaged, leading to much improved device properties and a higher success ratio for device fabrication.

CuPc is a cheap, commercially available pigment that not only has high thermal and chemical stability,<sup>[6]</sup> but also exhib-

[\*] Prof. W. Hu, Prof. D. Zhu, Q. Tang, Dr. H. Li, Y. Song, Dr. W. Xu, Prof. L. Jiang, Prof. Y. Liu  
Beijing National Laboratory for Molecular Sciences  
Key Laboratory of Organic Solids  
Institute of Chemistry, Chinese Academy of Sciences  
Beijing 100080 (P.R. China)  
E-mail: huwp@iccas.ac.cn; dbzhu@iccas.ac.cn  
Q. Tang, Y. Song  
Graduate School of Chinese Academy of Sciences  
Beijing 100039 (P.R. China)  
Prof. X. Wang  
Institute of Plasma Physics, Chinese Academy of Sciences  
230031, Hefei, Anhui (P.R. China)

[\*\*] WH is grateful to Prof. Chunli Bai (Chinese Academy of Sciences), Prof. Chen Wang (National Center for Nanoscience and Technology), Prof. Heidiaki Takayanagi (NTT Basic Research Laboratories), Prof. Christian Kloc (Bell Labs), Dr. Meng He (National Center for Nanoscience and Technology), Dr. Vitaly Podzorov (Rutgers University), and Dr. Esther Barrena (Max-Planck-Institut für Metallforschung) for profound discussions. WH is grateful to Dr. Meng He (National Center for Nanoscience and Technology) for English revision. The authors acknowledge financial support from the National Natural Science Foundation of China (20421101, 20571079, 20527001, 90401026, 20472089, 90206049), the Ministry of Science and Technology of China (Program 973, 2006CB806200) and the Chinese Academy of Science. Supporting Information is available online from Wiley InterScience or from the author.

its excellent photoelectrical properties, for example, field-effect properties.<sup>[7]</sup> Previously, we have synthesized single-crystalline sub-micrometer sized ribbons of CuPc on porous aluminum oxide membranes<sup>[8a]</sup> using a physical vapor transport technique.<sup>[8b]</sup> However, the success of the device fabrication was rather low because of the handpicking process used to transfer the sub-micrometer ribbons from porous aluminum oxide membranes to SiO<sub>2</sub>/Si substrates.<sup>[8a]</sup> Recently, we developed a new method for the in situ patterning of single-crystalline CuPc nanoribbons on an SiO<sub>2</sub> surface (300 nm in thickness) to avoid such problems.

The in situ patterning process of single-crystalline CuPc nanoribbons on an SiO<sub>2</sub> surface was carried out as follows: First, previously prepared CuPc single-crystalline sub-micrometer-sized ribbons were immersed in ethanol and sonicated to obtain a CuPc nanocrystal suspension. Then, Si/SiO<sub>2</sub> substrates, cleaned in advance using organic solvents and oxygen plasma, were dipped into the suspension to predeposit CuPc nanocrystals (Fig. 1a<sub>1</sub>) on their surface. The predeposited SiO<sub>2</sub>/Si substrates were then transferred into a physical vapor transport system to grow CuPc nanoribbons (Fig. 1a<sub>2</sub>). It is interesting that CuPc nanoribbons indeed grew from predeposited CuPc nanocrystals along the *b*-axis and extended along the surface of the substrate (Fig. 1b<sub>1</sub> and 1b<sub>2</sub>). The growth could start from one end (Fig. 1b<sub>1</sub>) or from both ends (Fig. 1b<sub>2</sub>) of the nanocrystal, and finally evolved into nanoribbons on the SiO<sub>2</sub> surface (Fig. 1c). In our experience, this method worked better when the size of the nanocrystals used to seed the growth of the nanoribbons was less than ca. 100 nm. Using larger crystal seeds resulted in the crystalline seeds standing vertically so that the patterning could not be achieved (see Supporting Information). Moreover, the growth was better when the density of the crystalline seeds was not too high, because the aggregation of the crystal seeds resulted in disorderly growth of nanoribbons (see Supporting Information), sometimes even perpendicular to the substrate.

The width of the patterned nanoribbons ranged from 40 to 150 nm and the length from a few micrometers to several tens of micrometers (Fig. 2a–e). Transmission electron microscopy

(TEM) observations indicated that these nanoribbons were  $\beta$ -CuPc and grew along the [010] direction (Fig. 2f<sub>1</sub> and f<sub>2</sub>), as found for previously synthesized sub-micrometer-sized ribbons.<sup>[8a]</sup> In the  $\beta$ -phase, CuPc molecules stack along the [010] direction<sup>[9]</sup> through strong  $\pi$ – $\pi$  interactions whereas adjacent molecule columns are linked only by weak van der Waals forces (Fig. 2f<sub>3</sub>). This was believed to be the reason why  $\beta$ -CuPc grew into long nanoribbons along the [010] direction. Moreover, in  $\beta$ -CuPc the (010) plane is believed to have a high surface free energy while the (100), (001), (20 $\bar{1}$ ), and (10 $\bar{1}$ ) planes<sup>[9]</sup> have low surface free energies; the significant difference between the surface free energies of the different crystallographic planes in a single crystal also leads to the generation of the 1D structure.<sup>[10]</sup>

In fact, although sub-micrometer CuPc ribbons are broken into nanocrystals in the ultrasonication process, the newly formed nanocrystals still prefer to have the longest dimension along the [010] direction. When these nanocrystals were deposited on the surface of substrates, the direction of the longest dimension, [010] in most cases, lies along the plane of the surface. Accordingly, the subsequently obtained nanoribbons grow along the surface with their [010] direction in the plane of the surface. Hence, it is understandable that the orientation

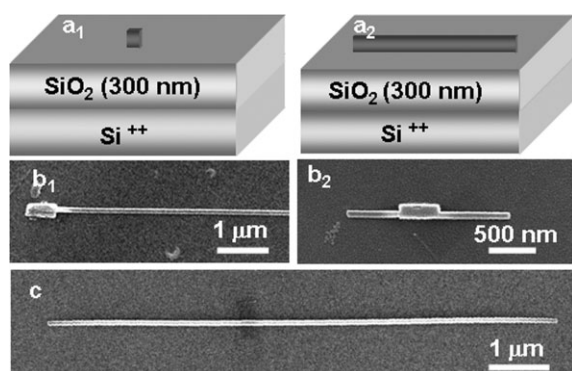


**Figure 1.** a<sub>1</sub>,a<sub>2</sub>) Illustrations showing that a pre-deposited CuPc nanocrystals on the SiO<sub>2</sub> surface develops into a nanoribbon. CuPc nanoribbons can grow from b<sub>1</sub>) one or b<sub>2</sub>) both ends of the pre-deposited nanocrystals. c) A patterned nanoribbon on the SiO<sub>2</sub> surface.

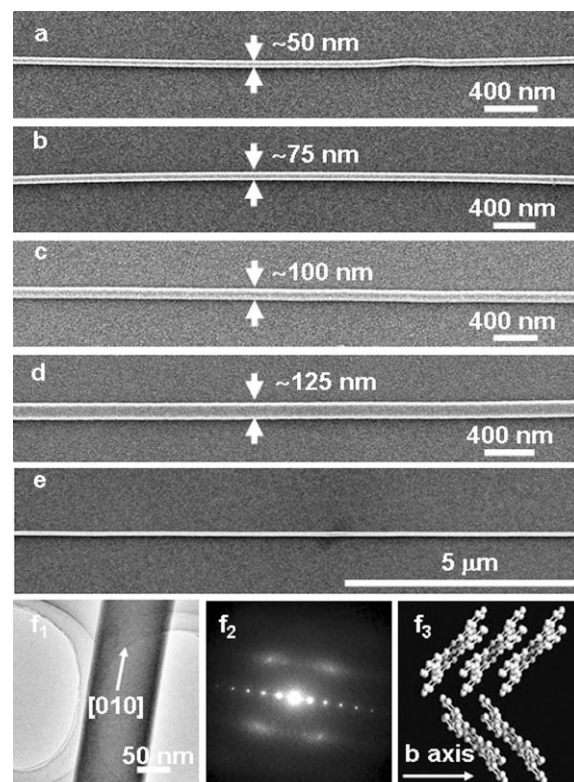


**Figure 2.** CuPc nanoribbons with different widths on a SiO<sub>2</sub> surface: a) ca. 50, b) ca. 75, c) ca. 100, and d) ca. 125 nm. e) The length of the nanoribbons ranges from several to several tens of micrometers. f<sub>1</sub>) Transmission electron microscopy (TEM) image and f<sub>2</sub>) selected area diffraction pattern indicating that the whole nanoribbon is a single crystal and grows along the [010] direction, in which CuPc molecules stack into columns (f<sub>3</sub>).

of the nanoribbons on the SiO<sub>2</sub> surface was dictated by that of the nanocrystals.

The orientation of the nanocrystals was strongly influenced by the method used to remove the substrate from the nanocrystal suspension. When the substrate was pulled out slowly and kept vertical during this process, the directions of the longest dimension of the nanocrystals, the [010] direction in most cases, were parallel to each other and in alignment with the direction in which the substrate was pulled from the suspension. The orientation of the nanocrystals could be adjusted further by a mechanical probe under an optical microscope or a probe tip in a scanning electron microscopy (SEM) system. Because the nanocrystals could be aligned, parallel nanoribbons could be prepared accordingly. We could also cut nanoribbons with a probe to make a new nanocrystal and then turn it in the plane of the substrate. With this method, we could obtain nanocrystals at any desired angle with respect to a particular nanoribbon. When the substrate was treated again in the physical vapor transport system, these nanocrystals grew into nanoribbons, and well-defined architectures could be obtained, as shown in Figure 3. The approach presented here could be used to construct integrated nanosystems and logic circuits<sup>[11]</sup> using organic single crystals. Recently, Rogers and co-workers<sup>[12]</sup> demonstrated an effective method for the patterning and manipulation of single-crystalline nanowires and microwires of GaAs into ordered arrays by the use of traditional photolithography and anisotropic, chemical wet etching. A printing technique using elastomeric stamps was used to transfer these wire arrays to plastic substrates with excellent retention of the order and crystallographic orientation of the wires. In principle, this method could be applied to our CuPc nanoribbons.

It is well known that the conduction channel of OFETs is located at the interface between the semiconductor and the SiO<sub>2</sub> gate insulator. Hence, the quality of the interface is crucial for OFETs. Our patterned nanoribbons were grown in situ on a SiO<sub>2</sub> surface in a physical vapor transport system. The

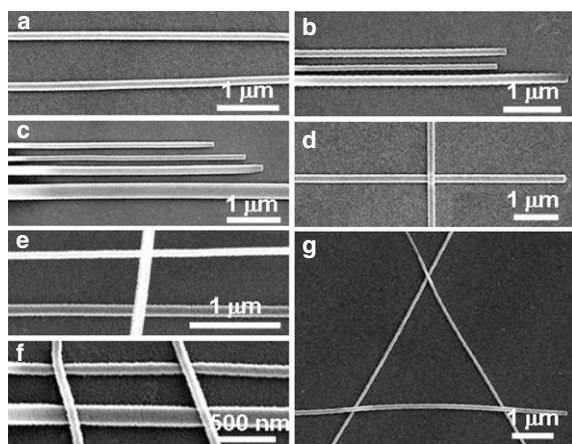


**Figure 3.** a–c) Parallel and d) crossed nanoribbons prepared by controlling the orientation of nanocrystals, and e–g) more complicated parallel or crossed architectures.

clean environment and the high substrate temperature excluded the possibility of interface pollution. Atomic force microscopy (AFM) was used to evaluate the nanoribbon/SiO<sub>2</sub> interface. As shown in Figure 4, the top surfaces of the nanoribbons were quite smooth (lines 1 and 2) and were strictly parallel to the substrate surface (line 3), indicating an intimate contact between the nanoribbons and the SiO<sub>2</sub> surface.

A series of OFETs based on patterned nanoribbons was fabricated, and typical ones are shown in Figure 5. The back of the low-resistance Si was used as the gate electrode. Typical output and transfer characteristics of our OFETs are given in Figure 6. The average mobility calculated in the saturated regime was ca. 0.1–0.4 cm<sup>2</sup> V<sup>−1</sup> s<sup>−1</sup> and the highest mobility was ca. 0.5 cm<sup>2</sup> V<sup>−1</sup> s<sup>−1</sup>. The threshold voltage and on–off ratio were −0.2 to ca. −0.6 V and 10<sup>4</sup> to 10<sup>5</sup>, respectively. The performance of our OFETs was much better than those made by the

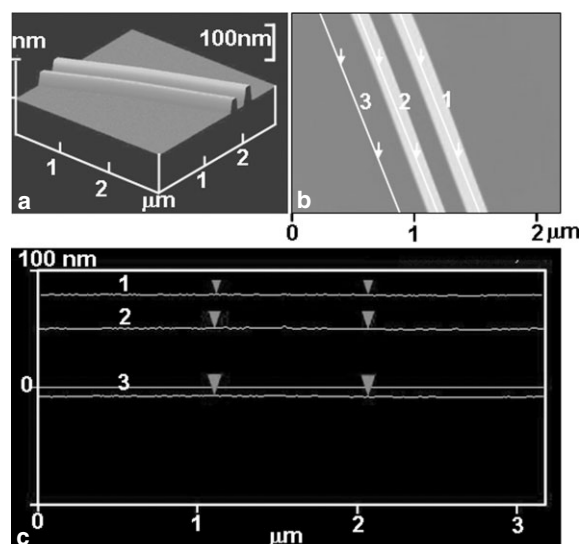


**Figure 4.** AFM images of patterned nanoribbons along the SiO<sub>2</sub> surface. The top surfaces of the nanoribbons were exactly parallel to the SiO<sub>2</sub> surface, i.e., CuPc nanoribbons had very close contact with the SiO<sub>2</sub> gate insulator. a) 3D image of in situ patterned CuPc nanoribbons, b) top image of CuPc nanoribbons, c) top surface line of CuPc nanoribbons (lines 1 and 2) shown to be parallel to the SiO<sub>2</sub> surface line (line 3).

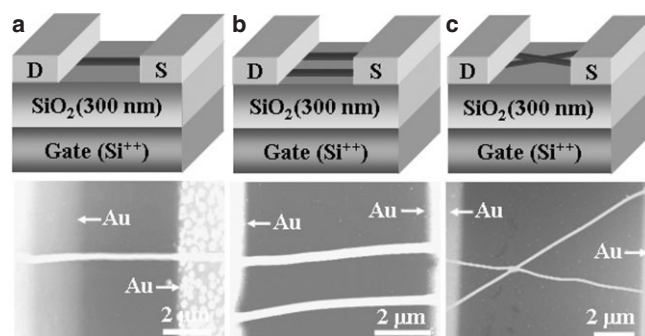


**Figure 5.** OFETs based on a) an individual patterned nanoribbon, b) parallel, and c) crossed architectures.

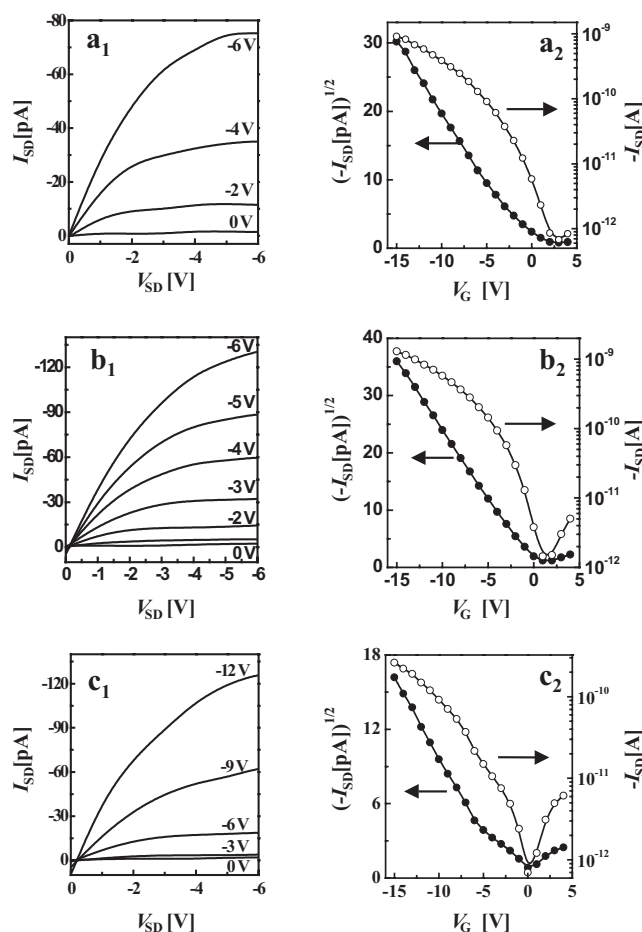


**Figure 6.** Typical output and transfer characteristics of OFETs based on a<sub>1</sub>,a<sub>2</sub>) single, b<sub>1</sub>,b<sub>2</sub>) parallel, and c<sub>1</sub>,c<sub>2</sub>) crossed nanoribbons. Transfer characteristics were measured at a fixed source–drain voltage,  $V_{SD} = -10$  V.  $I_{SD}$ : source–drain current,  $V_G$ : gate voltage.

handpicking process,<sup>[8a]</sup> suggesting that the in situ patterning technique is more suitable than the handpicking approach for OFET fabrication. Moreover, the transistor performance of our nanoribbons was of the same level as that of the bulk crystal of CuPc<sup>[7a]</sup> with an organic insulator (the highest mobility was ca.  $1 \text{ cm}^2 \text{ V}^{-1} \text{ s}^{-1}$  calculated in the saturated regime with an on–off ratio ca.  $10^4$ ; the insulator layer of the devices was parylene), which was much better than that of devices in thin films<sup>[7b,13]</sup> (mobility ca.  $0.02 \text{ cm}^2 \text{ V}^{-1} \text{ s}^{-1}$  calculated in the saturated regime with  $\text{SiO}_2$ <sup>[7b]</sup> or  $\text{PbZr}_{0.5}\text{Ti}_{0.5}\text{O}_3$ <sup>[13]</sup> as insulators).

In summary, a novel method has been demonstrated for the in situ patterning of organic single-crystalline nanoribbons on an  $\text{SiO}_2$  surface to obtain various architectures. OFETs based on the patterned nanoribbons exhibited a low threshold voltage and high carrier mobility, because the in situ patterning process is free from surface pollution, avoids damage of the single crystals, and provides a high-quality crystal/ $\text{SiO}_2$  interface. This method not only overcomes the general disadvantages of the handpicking process for the fabrication of organic single-crystal devices, but also provides a possibility for

making organic single-crystalline OFETs and nanoarchitectures on conventional  $\text{SiO}_2/\text{Si}$  substrates. Furthermore, this method opens up a new route for the fabrication of organic single-crystalline architectures and devices with very small crystals such as nanocrystals.

## Experimental

The substrates used in the present study were successively cleaned with pure water, hot acetone, pure ethanol, and argon plasma (about 15 s). A quartz tube was inserted in a two-zone horizontal tube furnace. CuPc powder was placed at the high-temperature zone and vaporized at  $425^\circ\text{C}$ . The CuPc vapor was then carried by high-purity Ar flowing from the high-temperature zone to the low-temperature zone at a rate of 200 sccm. Nanoribbons were obtained on a substrate with predeposited nanocrystals at the low-temperature zone ( $150^\circ\text{C}$ ). The current–voltage ( $I$ – $V$ ) characteristics of OFETs were recorded with a Keithley 4200 SCS and a Micromanipulator 6150 probe station in a clean and metallic shielded box at room temperature in air. SEM images were obtained with a Hitachi S-4300 SE (Japan), and TEM images were obtained with a JEOL 2010. AFM was performed with a Nanoscope IIIa (USA).

Received: March 15, 2006

Revised: July 5, 2006

- [1] a) R. F. Service, *Science* **2006**, *311*, 1691. b) G. Malliaras, R. Friend, *Phys. Today* **2005**, *58*, 53. c) I. McCulloch, *Nat. Mater.* **2005**, *4*, 583. d) E. Reichmanis, H. Katz, C. Kloc, A. Maliakal, *Bell Labs Tech. J.* **2005**, *10*, 87. e) A. Facchetti, M. H. Yoon, T. J. Marks, *Adv. Mater.* **2005**, *17*, 1705. f) H. Sirringhaus, *Adv. Mater.* **2005**, *17*, 2411. g) Y. Sun, Y. Liu, D. Zhu, *J. Mater. Chem.* **2005**, *15*, 53. h) T. W. Kelley, P. F. Baude, C. Gerlach, D. E. Ender, D. Muires, M. A. Haase, D. E. Vogel, S. D. Theiss, *Chem. Mater.* **2004**, *16*, 4413. i) A. Cravino, N. S. Sariciftci, *Nat. Mater.* **2003**, *2*, 360. j) J. L. Bredas, S. Marder, *Adv. Funct. Mater.* **2002**, *12*, 555. k) J. A. Rogers, Z. Bao, K. Baldwin, A. Dodabalapur, B. Crone, V. R. Raju, V. Kuck, H. Katz, K. Amundson, J. Ewing, P. Drzaic, *Proc. Natl. Acad. Sci. USA* **2001**, *98*, 4835.
- [2] a) G. Horowitz, B. Bachet, A. Yassar, P. Lang, F. Demanze, J. Fave, F. Garnier, *Chem. Mater.* **1995**, *7*, 1337. b) H. E. Katz, A. J. Lovinger, J. G. Laquindanum, *Chem. Mater.* **1998**, *10*, 457. c) V. C. Sundar, J. Zaumseil, V. Podzorov, E. Menard, R. L. Willett, T. Someya, M. E. Gershenson, J. A. Rogers, *Science* **2004**, *303*, 1644. d) V. Podzorov, V. M. Pudalov, M. E. Gershenson, *Appl. Phys. Lett.* **2003**, *82*, 1739. e) V. Podzorov, S. E. Sysoev, E. Loginova, V. M. Pudalov, M. E. Gershenson, *Appl. Phys. Lett.* **2003**, *83*, 3504. f) R. W. I. de Boer, M. E. Gershenson, A. F. Morpurgo, V. Podzorov, *Phys. Status Solidi A* **2004**, *201*, 1302. g) R. Zeis, C. Besnard, T. Siegrist, C. Schlockermann, X. L. Chi, C. Kloc, *Chem. Mater.* **2006**, *18*, 244.
- [3] A. L. Briseno, J. Aizenberg, Y. J. Han, R. A. Penkala, H. Moon, A. J. Lovinger, C. Kloc, Z. Bao, *J. Am. Chem. Soc.* **2005**, *127*, 12 164.
- [4] a) R. W. I. de Boer, T. M. Klapwijk, A. F. Morpurgo, *Appl. Phys. Lett.* **2003**, *83*, 4345. b) J. Takeya, C. Goldmann, S. Hass, K. P. Pernstich, B. Ketterer, B. Batlogg, *J. Appl. Phys.* **2003**, *94*, 5800. c) M. M. Torrent, M. Durkut, P. Hadley, X. Ribas, C. Rovira, *J. Am. Chem. Soc.* **2004**, *126*, 984.
- [5] H. Moon, R. Zeis, E. J. Borkent, C. Besnard, A. J. Lovinger, T. Siegrist, C. Kloc, Z. Bao, *J. Am. Chem. Soc.* **2004**, *126*, 15 322.
- [6] a) J. Simon, J. J. Andre, *Molecular Semiconductors*, Springer, Berlin **1985**. b) *Phthalocyanines: Properties and Applications*, Vol. 3, (Eds: C. C. Leznoff, A. B. P. Lever), VCH, Weinheim, Germany **1993**.

- [7] a) R. Zeis, T. Siegrist, C. Kloc, *Appl. Phys. Lett.* **2005**, *86*, 022103.  
b) Z. Bao, A. J. Lovinger, A. Dodabalapur, *Appl. Phys. Lett.* **1996**, *69*, 3066. c) G. Horowitz, *Adv. Mater.* **1998**, *10*, 365. d) J. Zhang, H. Wang, X. Yan, J. Wang, J. Shi, D. Yan, *Adv. Mater.* **2005**, *17*, 1191.
- [8] a) Q. Tang, H. Li, M. He, W. Hu, C. Liu, K. Chen, C. Wang, Y. Liu, D. Zhu, *Adv. Mater.* **2006**, *18*, 65. b) R. A. Laudise, C. Kloc, P. G. Simpkins, T. Siegrist, *J. Cryst. Growth* **1998**, *187*, 449.
- [9] a) J. M. Robertson, *J. Chem. Soc.* **1935**, 615. b) C. J. Brown, *J. Chem. Soc.* **1968**, 2488.
- [10] V. F. Puentes, K. M. Krishnan, A. P. Alivisatos, *Science* **2001**, *291*, 2115.
- [11] a) A. Bachtold, P. Hardley, T. Nakanishi, C. Dekker, *Science* **2001**, *294*, 1317. b) Z. H. Zhong, D. L. Wang, Y. Cui, M. W. Bockrath, C. M. Lieber, *Science* **2003**, *302*, 1377. c) R. S. Friedman, M. C. McAlpine, D. S. Ricketts, D. Ham, C. M. Lieber, *Nature* **2005**, *434*, 1085.
- [12] a) Y. G. Sun, J. A. Rogers, *Nano Lett.* **2004**, *4*, 1953. b) E. Menard, K. J. Lee, D. Y. Khang, R. G. Nuzzo, J. A. Rogers, *Appl. Phys. Lett.* **2004**, *84*, 5398.
- [13] T. Okuda, S. Shintoh, N. Terada, *J. Appl. Phys.* **2004**, *96*, 3586.